

## Surface Attachment of Protein Fibrils via Covalent Modification Strategies

Alexander K. Buell,<sup>†</sup> Duncan A. White,<sup>‡</sup> Christoph Meier,<sup>†</sup> Mark E. Welland,<sup>†</sup>  
Tuomas P. J. Knowles,<sup>†</sup> and Christopher M. Dobson<sup>\*,‡</sup>

Nanoscience Centre, University of Cambridge, 11 JJ Thomson Avenue, CB3 0FF, U.K., and Department of Chemistry, University of Cambridge, Lensfield Road, CB2 1EW, U.K.

Received: February 22, 2010; Revised Manuscript Received: July 7, 2010

Chemical control of surface functionality and topography is an essential requirement for many technological purposes. In particular, the covalent attachment of monomeric proteins to surfaces has been the object of intense studies in recent years, for applications as varied as electrochemistry, immuno-sensing, and the production of biocompatible coatings. Little is known, however, about the characteristics and requirements underlying surface attachment of supramolecular protein nanostructures. Amyloid fibrils formed by the self-assembly of peptide and protein molecules represent one important class of such structures. These highly organized  $\beta$ -sheet-rich assemblies are a hallmark of a range of neurodegenerative disorders, including Alzheimer's disease and type II diabetes, but recent findings suggest that they have much broader significance, potentially representing the global free energy minima of the energy landscapes of proteins and having potential applications in material science. In this paper, we describe strategies for attaching amyloid fibrils formed from different proteins to gold surfaces under different solution conditions. Our methods involve the reaction of sulfur containing small molecules (cystamine and 2-iminothiolane) with the amyloid fibrils, enabling their covalent linkage to gold surfaces. We demonstrate that irreversible attachment using these approaches makes possible quantitative analysis of experiments using biosensor techniques, such as quartz crystal microbalance (QCM) assays that are revolutionizing our understanding of the mechanisms of amyloid growth and the factors that determine its kinetic behavior. Moreover, our results shed light on the nature and relative importance of covalent versus noncovalent forces acting on protein superstructures at metal surfaces.

### Introduction

Many advances in the biological sciences and biotechnology, ranging from the characterization of molecular motors<sup>1</sup> and protein electrochemistry<sup>2</sup> to immunochemical assays,<sup>3</sup> the control of surface hydrophobicity,<sup>4</sup> and biosensing<sup>5</sup> involve the reliable attachment of proteins to surfaces. The length scales involved in the control of surface topography needed in these types of applications range from the size of a protein monomer (nm) to that of higher order multimolecular assemblies ( $\mu\text{m}$ ). A particular case where control of the surface attachment of supramolecular protein structures is of great practical importance is the study of the phenomenon of protein misfolding and aggregation. Misfolding can manifest itself as a self-assembly process leading to the formation of well-defined polymeric structures that are commonly known as amyloid fibrils; these species have increasing significance in fields as varied as molecular medicine and materials science.<sup>6</sup> This type of fibril was originally discovered in intra- or extracellular deposits in a range of medical conditions, most notably associated with neurodegenerative disorders such as Alzheimer's and Parkinson's disease.<sup>7,8</sup> In the past decade, however, an increasing number of peptides and proteins have been found either to possess the intrinsic propensity to form these structures under nonphysiological conditions,<sup>9</sup> or even to have been optimized by evolution to do so in order to exploit the remarkable structural properties of these fibrils.<sup>10,11</sup> A detailed study of the molecular

mechanisms of misfolding can therefore provide insights into the fundamental driving forces that govern the behavior of polypeptide molecules in nature<sup>12</sup> and the process of molecular evolution.

Whereas structural studies by methods such as nuclear magnetic resonance (NMR) spectroscopy,<sup>13</sup> X-ray diffraction,<sup>14</sup> cryo-electron microscopy,<sup>15</sup> or atomic force microscopy (AFM)<sup>16</sup> are applicable to the study of relatively deep minima of the free energy surface characterizing the degrees of freedom of a polypeptide chain, associated for example with the native state, folding intermediates, and the amyloid form of proteins, kinetic measurements are needed to gain insight into the energy barriers separating such minima. The extent to which variations in external conditions or differences in the intrinsic amino acid sequences influence the kinetics of amyloid assembly is a direct manifestation of the modified free energy surface. Two classes of kinetic measurement techniques can be distinguished. One is based on measurements carried out in bulk solution, e.g., monitoring the fluorescence emission by amyloidophilic dyes,<sup>17</sup> light scattering techniques,<sup>18</sup> or the time dependence of the circular dichroism of the protein solution.<sup>19</sup> The other, that has emerged over the past decade, involves techniques such as surface plasmon resonance (SPR)<sup>20,21</sup> and quartz crystal microbalance (QCM)<sup>22–27</sup> or microcantilever measurements,<sup>27,28</sup> where the growth of amyloid fibrils that are bound to a surface can be studied with unprecedented accuracy. If reliable and irreversible surface attachment can be achieved, the growth kinetics of a constant and well-defined ensemble of fibrils can be monitored during the whole time course of an experiment; this feature offers crucial advantages compared with many bulk solution measurements of molecular self-assembly, where a

\* To whom correspondence should be addressed. E-mail: cmd44@cam.ac.uk.

<sup>†</sup> Nanoscience Centre.

<sup>‡</sup> Department of Chemistry.

series of different samples must be studied and compared and where other factors such as fragmentation of the fibrils may influence the data. In addition to these practical considerations, the presence and influence of surfaces are of fundamental interest, not the least because living cells are compartments with very high specific internal surface areas. The small volume of a cell, which is packed with other macromolecules that act as “crowding agents”, leads to a very high surface-to-volume ratio compared to that found in experiments carried out in a test tube. The extent to which surfaces influence the various steps in the process of protein misfolding and aggregation is therefore a topic of much current debate.<sup>29,30</sup>

These considerations highlight the need for an approach where the attachment of amyloid fibrils to surfaces, in particular gold surfaces due to their widespread use in biosensing, can be carefully controlled. In most cases where attachment of a macromolecule to gold is required, the general approach is to use a linker molecule containing a thiol group and to exploit the high propensity of the latter to form a covalent gold–sulfur bond.<sup>31</sup> Subsequently, the attachment of amyloid fibrils or other protein structures to the layer of linker molecules can be achieved either via an amide coupling reaction<sup>20,21</sup> or through antibody–antigen interactions.<sup>25</sup> Both methods have been applied to amyloid fibrils under solution conditions (e.g., pH and temperature) where the particular fibrils under investigation are stable. Many fibrils, however, form from the soluble states of their component proteins only under relatively specific conditions, and preformed fibrils can dissociate if these conditions are changed.<sup>32</sup>

The common attachment methods for proteins rely on the fact that side chain amines and carboxylic acids are usually abundant. A fundamental challenge, however, is that the reactivity of these groups is highly dependent on the pH value of the solutions involved. Thus, for example, under acidic conditions, where many amyloidogenic proteins form fibrils particularly readily,<sup>33</sup> the amine groups are mostly protonated and the number of accessible nonprotonated nucleophilic amines available for amide coupling is very low. Extensions to these methodologies are therefore required to establish general methods that cover a wide range of pH values. In addition, it is also advantageous to enlarge the toolbox of available attachment chemistries, at neutral pH in particular, because, as we demonstrate below, given methods of surface attachment can have very different efficiencies for fibrils assembled from different proteins.

In this paper, we describe a novel strategy based on the attachment of small molecule linkers to protein fibrils of interest, followed by attachment of these protein nanostructures to gold surfaces. In addition, we demonstrate the applicability of this method for biosensor measurements of amyloid growth under solution conditions where there is a strong need for an irreversible covalent attachment process, rather than relying on noncovalent interactions between the metal surface and the amyloid fibrils.

## Experimental Section

**Atomic Force Microscopy (AFM).** All of the images shown in this paper were acquired with tapping mode in air using a Molecular Imaging PicoPlus (Tempe, AZ) atomic force microscope (AFM). For the images in Figure 1, nonsonicated amyloid fibrils were deposited on cleaved mica substrates. The substrates for the images in Figure 8 were prepared as described below. All of the other images show amyloid fibrils on the surfaces of

commercially available quartz crystal microbalance biosensors (Q-Sense QSX 301, Västra Frölunda, Sweden).

**Amyloid Fibril Growth.** The proteins used for the formation of amyloid fibrils were either expressed according to standard protocols (human  $\alpha$ -synuclein,<sup>34</sup> bovine PI3K-SH3<sup>9</sup> and its M1C mutant) or purchased from commercial suppliers (bovine insulin and its B-chain, hen egg white and human lysozymes, bovine  $\beta$ -lactoglobulin, bovine and human  $\alpha$ -lactalbumins, from Sigma Aldrich, Dorset, U.K., and  $A\beta$  (1–42) from Bachem, Basel, Switzerland) and used without further purification. The transformation of the soluble monomeric proteins into insoluble amyloid fibrils also followed the published protocols in each case: PI3K-SH3,<sup>9</sup>  $\alpha$ -synuclein,<sup>35</sup> bovine insulin,<sup>22</sup> insulin B-chain,<sup>36</sup> hen egg white<sup>37</sup> and human lysozyme,<sup>38</sup> bovine  $\beta$ -lactoglobulin,<sup>39</sup> and  $\alpha$ -lactalbumin.<sup>40</sup> All fibril samples were stored at room temperature.

**Fibril Modification under Acidic Conditions.** The detailed protocol for modifying fibrils at low pH is illustrated for PI3K-SH3; the modification of bovine  $\beta$ -lactoglobulin, the  $\alpha$ -lactalbumins, and the lysozymes was carried out in an essentially identical manner. 100  $\mu$ L aliquots of 1 mM fibril solution at pH 2.0 were mixed with 100  $\mu$ L of 1 M cystamine dihydrochloride (Sigma) solution and 1 mg of EDC (*N*-(3-dimethylaminopropyl)-*N'*-ethylcarbodiimide hydrochloride, Sigma), and then made up to 2 mL with HCl, pH 2.0. The solution was centrifuged at 20 °C for 2 h at 12 krpm (ca. 8500 g), the supernatant removed, and the remaining pellet redissolved in 2 mL of HCl, pH 2.0. This procedure was carried out three times in order to minimize any excess cystamine which could compete with the fibrils for surface attachment. The final pellet was resuspended in 500  $\mu$ L of HCl at pH 2. In order to calculate the remaining cystamine and EDC in the final fibril suspension, it was assumed that in every centrifugation step 90% of these reagents were removed together with the supernatant (from estimated relative volumes of pellet and supernatant).

**Fibril Modification under Physiological Conditions.** For  $\alpha$ -synuclein, 50  $\mu$ L aliquots of a ca. 100  $\mu$ M solution of the fibrillar form of the protein were diluted with water to 1 mL and then 1 mg of 2-iminothiolane (Traut's reagent) was added. The solution was then left to react for at least 5 min. The extent to which the fibrils are modified depends on the relative concentration of Traut's reagent and the time of incubation. In fact, 2 h of incubation of the  $\alpha$ -synuclein fibrils with Traut's reagent led to complete disappearance of the unmodified peak in the mass spectrum. For  $A\beta$  (1–42), 100  $\mu$ L aliquots of approximately 30  $\mu$ M solutions of amyloid fibrils formed from  $A\beta$  (1–42) in PBS buffer were centrifuged at 90 krpm for 1 h. The supernatant was removed, and the remaining sample (no pellet was visible) was resuspended in 200  $\mu$ L of water. The fibril solutions were then reacted with 1.5  $\mu$ g of 2-iminothiolane for ca. 15 min.

**Elongation of Seed Fibrils with Modified Monomeric Protein.** A solution of 10 mg (0.7  $\mu$ M) of hen lysozyme in 1 mL of 100 mM phosphate buffer (pH 7.5) was prepared; then, 10  $\mu$ L of 3 mg (22  $\mu$ mol) of 2-iminothiolane (Sigma-Aldrich) dissolved in 100  $\mu$ L of 100 mM phosphate buffer (pH 7.5) was added. The solution was incubated for 1 h at RT and then acidified to pH 2 with 210  $\mu$ L of 1 M HCl and incubated at 65 °C for 6 days. A 1 mg portion of the B-chain of bovine insulin was diluted in 700  $\mu$ L of H<sub>2</sub>O. First, 20  $\mu$ L of 100 mM phosphate buffer (pH 7.4) and then 4 equiv of Traut's reagent were added. After 5 min, the reaction was quenched with 10  $\mu$ L of 1 N HCl. To seed the fibril formation, 20  $\mu$ L of preformed

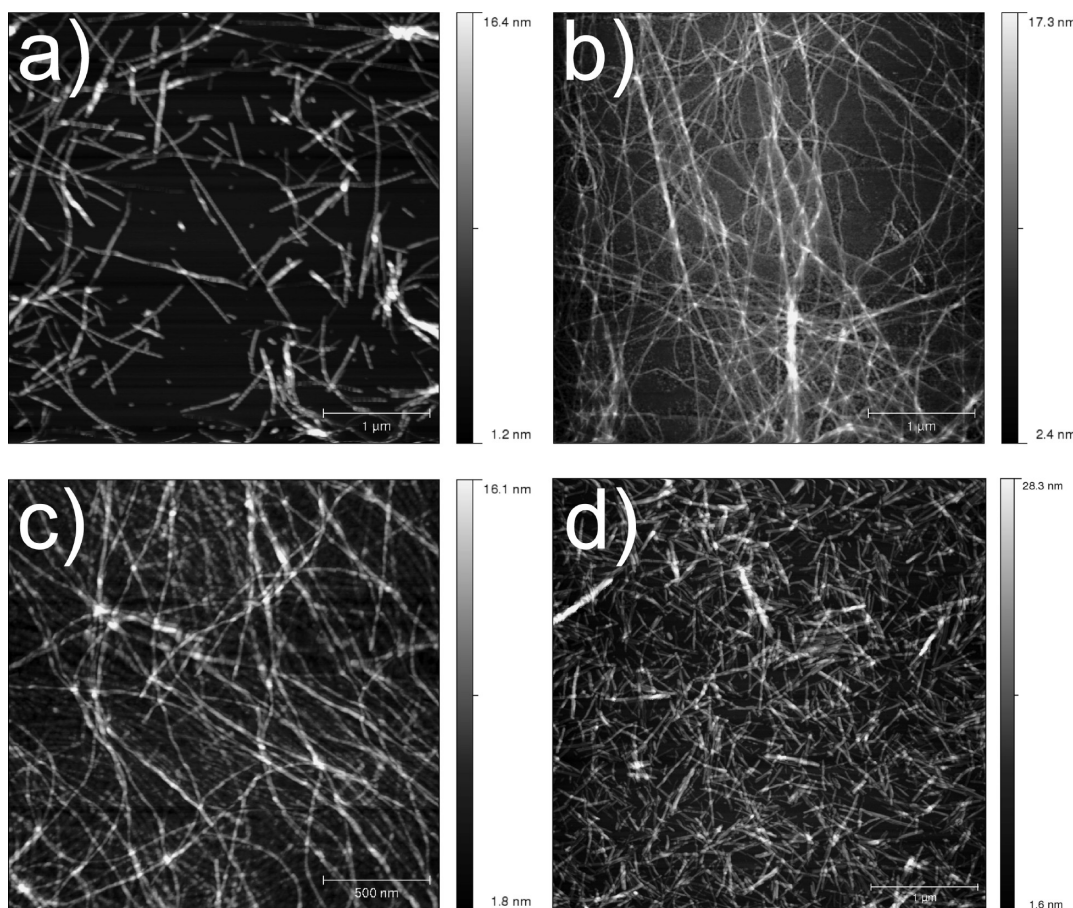


**Figure 1.** AFM images of amyloid fibrils from different proteins, that were grown according to the protocols given in the Experimental Section: (a) bovine insulin; (b) hen lysozyme; (c) the M1C mutant of PI3K-SH3; (d) the B-chain of bovine insulin (images on cleaved mica substrates; fibril solution dried in, not rinsed away).

(see above) unmodified B-chain fibrils was added to the monomer solution which was then stirred overnight at 30 °C.

**Mass Spectrometry.** The activated amyloid fibrils were dissociated either via abrupt changes in pH (2.0 to ca. 12.0 in the case of PI3K-SH3 and 7.4 to ca. 0.5 in the case of  $\alpha$ -synuclein) or via suspension in DMSO ( $\alpha$ -synuclein) and then examined by mass spectrometry. The protein samples were purified from buffer salts and excess reagents with Ziptip C18 (Millipore, MA) and eluted in 50% acetonitrile and 0.1% formic acid. 2  $\mu$ L samples were electrosprayed from a gold-coated borosilicate capillary (Proxeon, Odense, Denmark). Mass spectra were recorded on a QSTAR Pulsar instrument (Applied Biosystems, Foster City, CA) with a capillary voltage of 1200 V and declustering potentials of 45 and 15 V. Deconvoluted protein spectra were generated using Bioanalyst software (Applied Biosystems).

Interestingly, in the initial experiments, no full length  $\alpha$ -synuclein (14.5 kDa) was observable in the reaction mixture by mass spectrometry, but instead, the dominant signals came from an 11.3 kDa species, indicative of a truncated form of the protein. This result is attributable to the fact that the fibrils had been maintained at room temperature for several weeks. Indeed, unmodified fibrils from the same batch that were dissociated in an identical manner also showed only the 11.3 kDa peak, associated with a peptide fragment of  $\alpha$ -synuclein. Similar truncation of peptide sequences during amyloid fibril formation has been reported for other fibril forming proteins.<sup>41,42</sup> Mass spectra of the pure monomeric protein, as well as of freshly prepared and dissociated fibrils, however, each showed a single

peak around 14.5 kDa (not shown), in good agreement with the theoretical mass of monomeric  $\alpha$ -synuclein (14.460 kDa), demonstrating that the strongly acidic conditions used to dissociate the fibrils can be used without cleavage of the sequence and showing that full length modified  $\alpha$ -synuclein fibrils could be prepared. The spectrum in Figure 5, acquired one day after the functionalization reaction was quenched by the drop in pH, was chosen as an illustration, because it shows that the attached 2-iminothiolane had essentially completely undergone the recyclization described in the Results section ( $\Delta M = 84$  Da).

**Attachment of Activated Fibrils to the Biosensor Surface.** **Attachment under Acidic Conditions.** The only step that differs in the protocols used for the various proteins that form amyloid fibrils particularly readily under acidic conditions is the duration of the ultrasonication that results from the different mechanical stability of the fibrils formed from different proteins. Different numbers of identical cycles with 3 s pulses and 3 s breaks were used (20% amplitude on a 500 W ultrasonic homogenizer, Cole Parmer, Hanwell, UK), and the total sonication times were as follows: insulin, 10 min; insulin B-chain, 2 min; PI3K-SH3, 30 s; lysozymes, 15 s;  $\beta$ -lactoglobulin, 3 s;  $\alpha$ -lactalbumins, 3 s. 100  $\mu$ L aliquots of each fibril solution were then pipetted onto a biosensor surface that was kept in an atmosphere with 100% humidity. Then, the surfaces were rinsed with HCl, pH 2.0, and the sensors were either inserted into the QCM for measurement or dried for AFM imaging. No additional passivation layers were required in this protocol, as we found that nonspecific attachment was small even after the first incubation of a biosensor with

monomeric protein, suggesting that the excess cystamine forms a charged layer that is very effective in preventing monomeric protein from nonspecific attachment.

**Attachment under Physiological Conditions.** The gold surfaces of biosensors were incubated for 1 h in an atmosphere of 100% humidity with 100  $\mu\text{L}$  of a solution containing freshly activated  $\alpha$ -synuclein fibrils that had been sonicated for a total of 4 min. The chips were then rinsed with water. Even though Traut's reagent has been shown to have a slow hydrolysis rate at neutral pH,<sup>43</sup> the high molar excess of the compound will lead to a partial coverage of the surface by its hydrolysis product, a thiol amide. In order to ensure complete passivation for the biosensor measurements, however, we incubated the surfaces with a 0.5 vol % solution of an inert PEG thiol ( $\text{CH}_3\text{O}(\text{CH}_2\text{CH}_2\text{O})_6\text{SH}$ , Polypure, Oslo, Norway) for 1 h, also at 100% humidity. Then, the chips were rinsed with water and dried for AFM imaging. In the case of A $\beta$  (1–42), the fibrils already had a length distribution appropriate for a biosensor measurement, and no sonication step was therefore required. A clean biosensor was incubated with 100  $\mu\text{L}$  of the solution of resuspended fibrils for 1 h in an atmosphere of 100% humidity. The sensor surface was rinsed with water and dried for AFM imaging.

**Preparation of Gold Surfaces with Different Roughnesses.** Template-striped gold (rms roughness ca. 0.5 nm) was produced as described previously.<sup>44</sup> Rough gold surfaces (rms roughness ca. 1.5 nm) were prepared by evaporating onto a freshly cleaved mica surface an adhesion layer of 2 nm of chromium followed by 100 nm of gold using a BOC Edwards Auto 306 evaporator (Crawley, U.K.). The biosensors used had a variable roughness between 0.8 and 2 nm, the largest roughness being observed for sensors after cleaning (see below).

**Quartz Crystal Microbalance (QCM) Measurements.** 1 mL of a 100  $\mu\text{M}$  solution of unmodified PI3K-SH3 amyloid fibrils was sonicated for 1 min (in 3 s pulses), and then, a biosensor was incubated with the resulting solution for 1 h. The gold surface was rinsed with HCl at pH 2.0 and then incubated with a 0.5 vol % solution of PEG thiol ( $\text{CH}_3\text{O}(\text{CH}_2\text{CH}_2\text{O})_6\text{SH}$ , Polypure, Oslo, Norway) for 1 h (pH also adjusted to 2.0). Then, the sensor was introduced into the microbalance and equilibrated overnight in HCl at pH 2.0. We used a D300 instrument (Q-Sense, Västra Frölunda, Sweden) to monitor the frequency shifts; the fundamental resonant frequency (5 MHz) and several of its harmonics ( $n = 3, 5, 7$ ) were recorded simultaneously. The sensors used were QSX 301-Standard Gold crystals (Q-Sense, Västra Frölunda, Sweden) with a frequency/mass sensitivity coefficient of 17.7 ng/cm<sup>2</sup> per Hz. The temperature in the 80  $\mu\text{L}$  chamber was controlled to within 0.05 °C. When a stable baseline had been established, the measurements shown in Figure 8a were performed; the measurements shown in Figure 8b were carried out with a biosensor loaded with fibrils that had cystamine molecules attached according to the procedures described above. For the NaCl concentration series in Figure 8c, the covalently attached PI3K-SH3 fibrils were successively exposed to solutions containing 4  $\mu\text{M}$  protein and increasing concentrations of NaCl. To stop the growth, the cell was flushed with 0.01 M HCl after each measurement. The total ionic strength of the protein solutions was calculated from the sum of the contribution of the HCl plus the added NaCl. The contribution of the protein molecules to the total ionic strength was neglected, as the protein concentration is more than 3 orders of magnitude lower than the salt concentrations.

**Cleaning of Biosensors.** The gold coated QCM chips to which amyloid fibrils were attached in this study were cleaned

and reused. To remove the protein fibrils, the crystals were immersed in 7 M sodium hydroxide solution at 80 °C for 2 h. The self-assembled monolayers (SAM) of either PEG thiol or cystamine on the gold surface were removed electrochemically.<sup>45</sup> A voltage of -2 V was applied to the gold surface of the crystal for ca. 1 min against a gold counter electrode in 100 mM phosphate buffer. The chips were then rinsed with distilled water and dried with nitrogen for reuse.

## Results and Discussion

In this paper, we discuss surface affinities and describe attachment strategies for mesoscale structures with diameters in the 2–10 nm range and lengths of the order of hundreds of nanometers or more. Examples of full length fibrils (up to several  $\mu\text{m}$  in length) as they form in solution are shown in Figure 1. In order to maximize control and comparability of the attachment experiments, we decreased the average fibril lengths via sonication (compare Figures 1 and 2), a procedure that leads to a more homogeneous length distribution and to a better distribution of the fibrils on the substrate. In addition, it facilitates suspension of the fibrils prior to deposition and, in the light of applications of our attachment methods in biosensing experiments, it maximizes the number of potential growth sites per mass of protein.

In the following sections, we present attachment methods under the two principal sets of pH conditions that are commonly used to generate amyloid fibrils, acidic (due to its destabilizing effect on folded proteins that facilitates the formation of fibrils) and physiological (due to its biological relevance). After briefly presenting an attachment method involving naturally occurring cysteine residues, applicable under both acidic and neutral conditions, we discuss strategies that involve modification of the polypeptide chains. Furthermore, we demonstrate the advantage of an irreversible covalent attachment strategy for applications in biosensing.

**Fibril Attachment via Naturally Occurring Cysteine Residues.** Attachment of amyloid fibrils to gold surfaces is straightforward and largely independent of solution pH when cysteine residues or disulfide bridges are present in the polypeptide sequence, provided they are exposed on the surface of the fibril. The attachment efficiency is not likely to depend on the formation of disulfide links by the cysteine residues, even though it still is a topic of debate as to whether a disulfide bond remains intact when attached to gold or whether it is cleaved.<sup>46,47</sup> We have previously used this strategy and shown its efficiency in the case of amyloid fibrils formed from bovine insulin<sup>22</sup> (see Figure 2a) that contains three disulfide bonds in its native state. Hen lysozyme can form amyloid fibrils under similar solution conditions to insulin and possesses two additional cysteine residues, 8 in total, all present as disulfide bonds in the native state in solution. However, the surface coverage that can be achieved by simple incubation is generally lower for lysozyme than for insulin, when incubated at the same fibril concentration for the same length of time; this low coverage is indicative of weaker binding, and the latter suggests that the cysteine residues in the lysozyme fibrils are less accessible for attachment than those in the insulin fibrils (2b). A similar observation holds for bovine  $\alpha$ -lactalbumin (2d), a structural homologue of lysozyme, and for a cysteine mutant of the PI3K-SH3 domain (2c), a protein which contains no cysteine residues in its natural sequence.

The covalent links between the fibrils and the gold surfaces are sufficiently stable such that the fibrils are not displaced from the surface even, for example, following a subsequent incubation

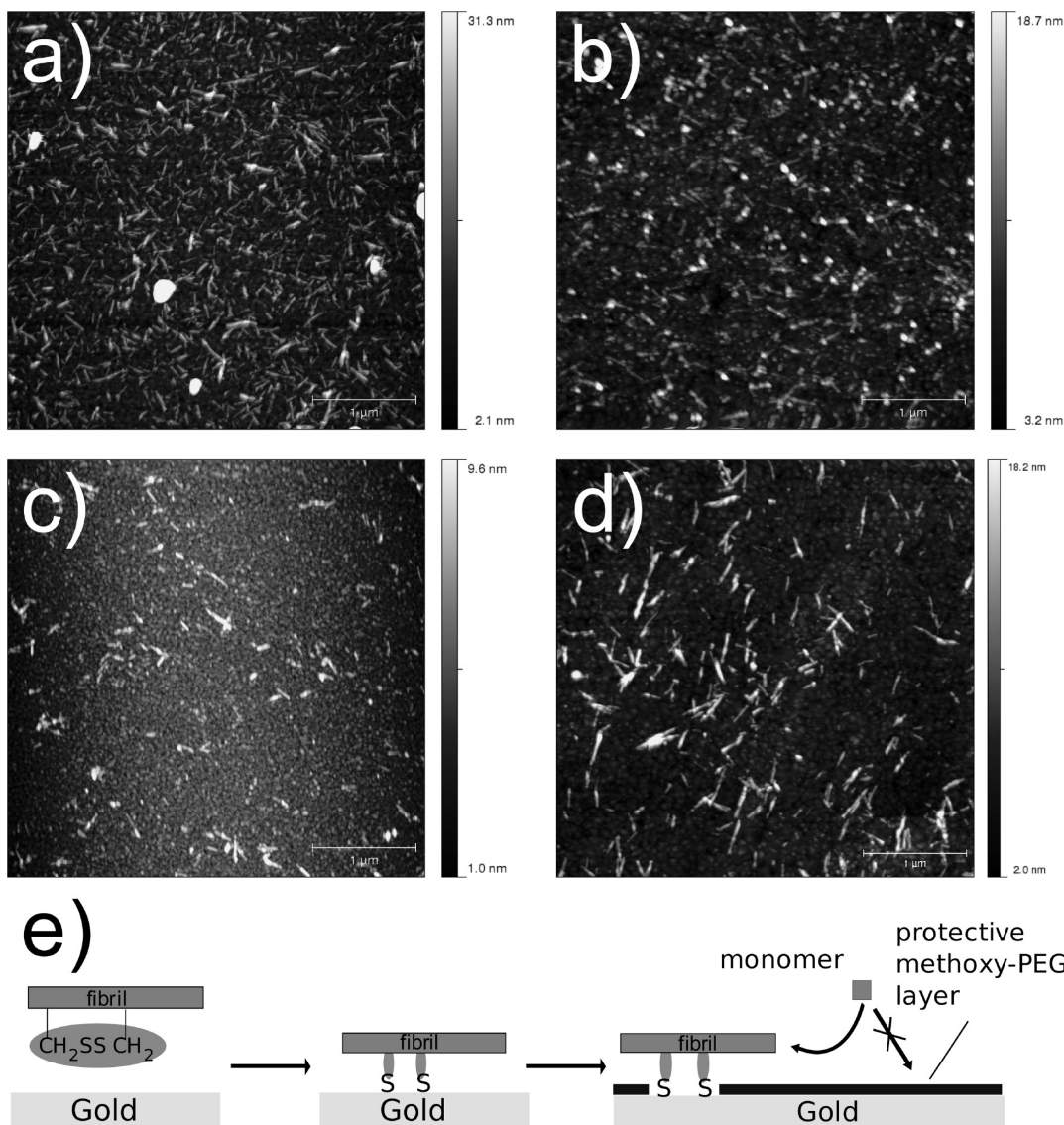


**Figure 2.** Attachment of amyloid fibrils from proteins containing cysteine/disulfide bridges in the amino acid sequence. In the case of bovine insulin (a), good surface coverages can be achieved<sup>22</sup> with this strategy. However, hen lysozyme (b), although having eight cysteine residues compared to six for insulin, attains a much lower surface coverage under similar experimental conditions, suggesting that the cysteines are largely buried inside the fibrils. Low surface densities of fibrils were also observed for a mutant of PI3K-SH3, where a cysteine residue has been artificially introduced (M1C) (c), as well as for bovine  $\alpha$ -lactalbumin (d), containing natural cysteines. Image size in all cases  $4 \times 4 \mu\text{m}^2$ . (e) Schematic diagram of cysteine attachment, including the subsequent passivation of the remaining gold layer.

with a thiol that forms self-assembled monolayers (SAMs) on gold surfaces (Figure 2e). This requirement is important for the attachment process, as the production of such a SAM on the regions of the surface not occupied by the fibril ends is important for biosensor measurements.<sup>22</sup> In particular, in the absence of such a layer, monomeric proteins are frequently capable of attaching directly onto the exposed gold surface, making it difficult to dissect the measured signal into the parts stemming from fibril elongation and from direct surface attachment of the monomeric building blocks.

**Fibril Modification under Acidic Conditions.** In order to control the attachment of amyloid fibrils formed from proteins without natural cysteine residues to surfaces in acidic solution, minimally invasive chemical modification of preformed fibrils offers a convenient strategy. Low pH conditions are known to be favorable for the *in vitro* preparation and study of many amyloidogenic proteins, and it has been suggested that similar conditions, for example, as a result of oxidative stress, could stimulate fibril formation *in vivo*.<sup>48</sup> Acidic conditions can present

a particular difficulty for any reaction involving protein functional groups, however, because any basic amino groups within a polypeptide chain (at the N-terminus or the side chains of lysine residues) are largely protonated and therefore not nucleophilic. Furthermore, the typically small quantity of amyloid fibrils that can be suspended acts to limit the maximal concentration of peptide amine groups in solution, resulting in a low attachment efficiency. In order to circumvent this problem, we have developed a strategy that is based on the well established attachment of cystamine [ $\text{H}_2\text{N}(\text{CH}_2)_2\text{SS}(\text{CH}_2)_2\text{NH}_2$ ] molecules to monomeric proteins,<sup>49</sup> where the aim is to introduce sulfhydryl groups into a specific molecular system (Figure 3). Reductive cleavage of the disulfide bonds within the attached cystamine molecule to form free thiol groups was omitted in the case of the fibrils, as disulfides appear to be as capable as free thiols of attaching to gold surfaces as discussed above.

The pH optimum for the initial step in the coupling reaction, the activation of carboxylic acid groups with *N*-(3-dimethylaminopropyl)-*N'*-ethylcarbodiimide hydrochloride (EDC), is at

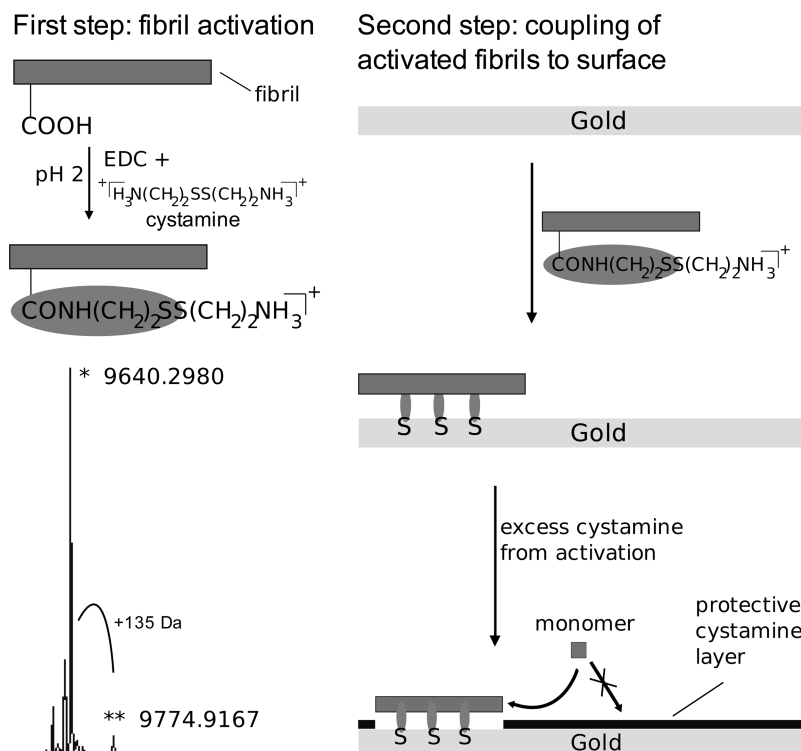


**Figure 3.** Schematic diagram of the surface attachment strategy (described in the Experimental Section) that was used under acidic conditions where many proteins readily form amyloid fibrils.<sup>33</sup> The method uses a large excess of cystamine because almost the entire population of amine groups is protonated at pH 2. This fact explains the low yield ( $\leq 5\%$ ) of functionalized molecules, as shown in the mass spectrum. (\*) is native protein, (\*\*) corresponds to protein molecules carrying one cystamine molecule.) Nevertheless, even this level of modification enables stable interactions of the amyloid fibrils with the surface to be achieved.

low pH values<sup>50</sup> as protonated carboxylic acids and not carboxylate ions attack the EDC. Nevertheless, acidic conditions are generally unfavorable for the formation of an amide bond as a result of the low reactivity of amines at pH values several units below the normal range of  $pK_a$  values of amine groups (ca. 9–11). Under these conditions, only a small fraction of these functional groups is unprotonated and therefore nucleophilic enough to attack an activated carboxylate group before it is hydrolyzed. This problem can be circumvented, however, with the approach described here, as a large excess of cystamine can be used to promote the coupling reaction. However, even by using excess cystamine, the fraction of carboxylic acid groups in a given protein that reacts with cystamine molecules is small. Indeed, in the case of PI3K-SH3, only ca. 5% of the polypeptide molecules within a fibril are modified (see mass spectrum in Figure 3 and the Experimental Section for details; estimates of relative populations based on the assumption of equal ionization efficiencies). Qualitative examination of mass spectra acquired from dissociated activated fibrils of other proteins ( $\beta$ -lactoglobulin, hen lysozyme) indicated similarly small reaction yields. Even though the yields are limited, they are sufficient to achieve efficient surface attachment of the fibrils because not every protein molecule within the polymeric assembly needs to interact with the surface. Moreover, as the cystamine molecules can react only with those carboxylic acid groups that are exposed on the surface of the fibrils, the disulfide bonds that have been coupled to the fibrils are likely to be in ideal positions to interact with the gold surface as soon as the modified fibril fragments diffuse toward it. The number of available carboxylic acid groups per unit length of fibril is likely to be variable between different proteins, as a result of differences in the number of acidic amino acids in the sequence and of different fractions of such residues that are exposed on the fibril surface. In the present study, for

example, the surface coverage achieved varied from a value of the order of  $20 \mu\text{m}^{-2}$  for bovine  $\alpha$ -lactalbumin to one of ca.  $100 \mu\text{m}^{-2}$  for hen lysozyme (see Figure 4 and Table 1). Indeed, in the case of the B-chain of insulin, mass spectrometric analysis could not identify a population of cystamine-containing molecules and, in agreement with this observation, no statistically significant increase in surface coverage was achieved relative to that obtained with unmodified fibrils (not shown). In this 30-residue peptide, the naturally occurring cysteine residues had been oxidized to sulfonic acids that are unable to form covalent bonds with gold. The small number of carboxylic acid groups in this short sequence, two side chains and the C-terminus all of which are potentially buried in the fibril core, appears to be unable to react with the cystamine groups to a significant extent under these reaction conditions. In all cases, the presence of unmodified fibrils on the gold surface even after rinsing (see e.g. Figure 7d) can be attributed to adsorption resulting from noncovalent interactions; this phenomenon will be discussed in detail in the last section of this paper. The excess of cystamine and the hydrolysis products of EDC generated during the reaction need to be removed after the reaction is complete, and this was achieved by repeated centrifugation and resuspension cycles to isolate the now modified fibrils from the reaction medium. In our experiments, fibril purification was terminated at a stage where approximately  $10\text{--}50 \mu\text{M}$  cystamine remained in solution (see the Experimental Section) with the fibrils, as the residual cystamine molecules provide a source of a self-assembled monolayer (SAM) on the unreacted gold surface, analogous to the polyethylene glycol (PEG) layer produced in the case of attachment of fibrils via cysteine residues.

In conclusion, we find that this method of covalent attachment of cystamine molecules to pregrown fibrils can increase the surface coverages attained for the majority of amyloid fibrils

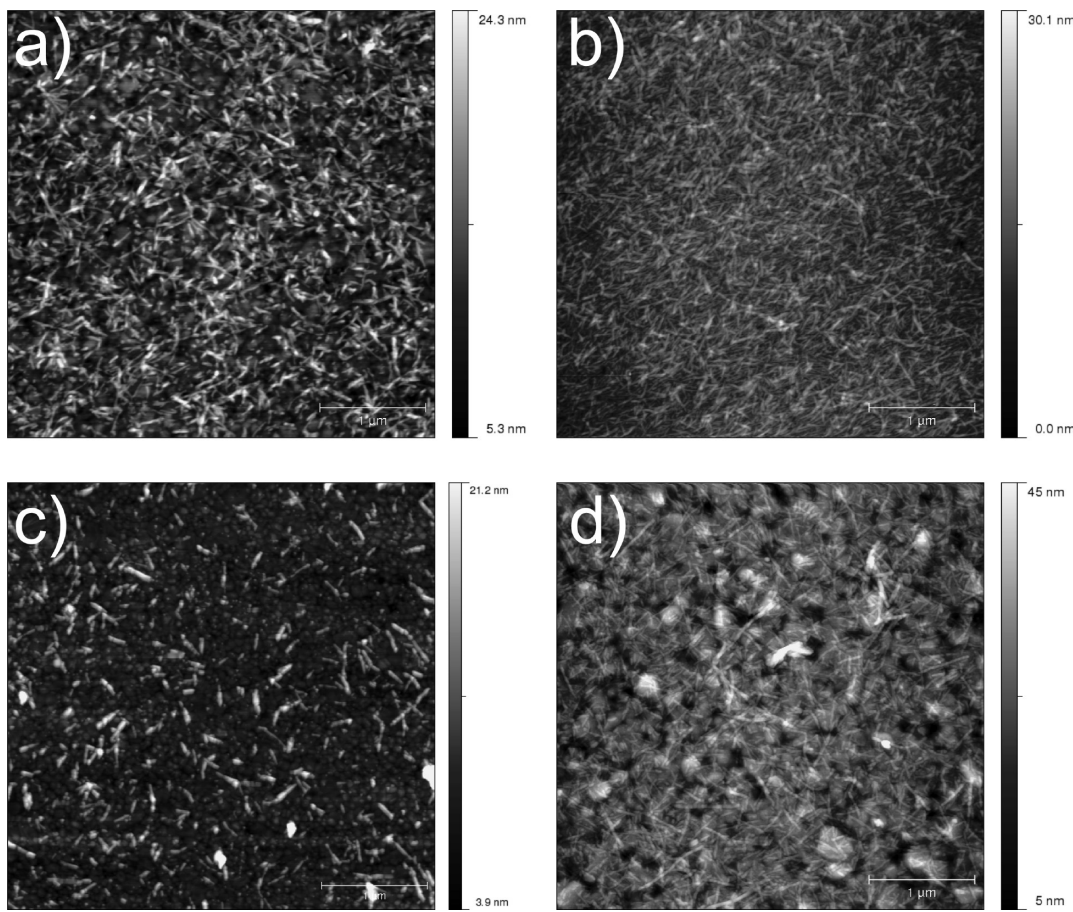


**Figure 4.** The attachment strategy presented in Figure 3 used for a range of amyloid fibrils formed at acidic pH. Examples are shown where sonicated (for details, see the Experimental Section) fibrils of (a) PI3K-SH3, (b) hen lysozyme, (c) bovine  $\alpha$ -lactalbumin, and (d) bovine  $\beta$ -lactoglobulin were functionalized and attached to gold surfaces of QCM chips. The surface coverages achieved in this way, as well as their increase compared to nonfunctionalized fibrils, varied greatly between the different proteins. This result is likely to be a consequence of variations in the number and accessibility of carboxylic acid groups in the amyloid fibrils under study, as these groups are first activated by EDC and subsequently react with the added cystamine.

**TABLE 1: Summary of Attachment Methods for the Proteins under Study<sup>a</sup>**

protein	pH	method	surface coverage enhancement factor
bovine insulin	2	natural cysteine attachment <sup>22</sup>	no modification required to achieve high surface coverage
bovine PI3K-SH3	2	attachment via cystamine	>10
HEW/human lysozyme, bovine $\beta$ -lactoglobulin, bovine/human $\alpha$ -lactalbumin	2	attachment via cystamine	2–5
human A $\beta$ (1–42), human $\alpha$ -synuclein	7.4	attachment via Traut's reagent	5–10
bovine insulin B-chain	7.4/1.0	premodification of monomer with Traut's reagent, subsequent elongation of seed fibrils with modified monomer	ca. 3–5

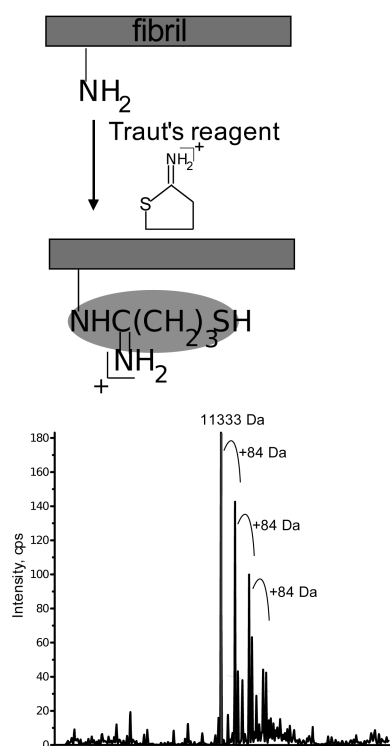
<sup>a</sup> The surface coverage enhancement due to the covalent modification of fibrils is reported as a comparison between an incubation of the gold surface with a solution of modified and non-modified fibrils and extensive rinsing of the surface with the respective (buffer) solution: PBS for A $\beta$  42 and  $\alpha$ -synuclein, pH 2.0 HCl for all the others.

generated from a range of different proteins compared to the surface coverages achieved with the nonmodified fibrils (compare Figures 2 and 4, and see Table 1) under identical acidic conditions. The increase in surface coverage between the unmodified and modified fibrils is largest in cases where no cysteines are present (e.g., PI3K-SH3). However, even in cases where cysteine residues are naturally present, the increase in surface density of fibrils can be a factor of 2 or more as a result of the fibril modification process, reducing the quantity of protein needed for a given coverage. In addition, if a higher number of fibrils per unit surface is achieved, it will lead to higher signal-to-noise levels in experiments involving the study

of the surface bound fibrils, especially in the case of species with a lower propensity to convert from the soluble into the fibrillar state.

**Fibril Modification under Physiological Conditions.** As discussed in detail above, if accessible natural cysteine residues are present in a sequence, amyloid fibrils could be attached to a surface via those thiol groups. Many amyloidogenic proteins, however, especially naturally unfolded polypeptides such as the A $\beta$  peptide and  $\alpha$ -synuclein that are implicated in disease, do not have cysteines in their sequence. The strategy that has been applied almost exclusively to date to attach amyloid fibrils under physiological conditions to gold surfaces is the coupling of

## First step: fibril activation



## Second step: coupling of activated fibrils to surface

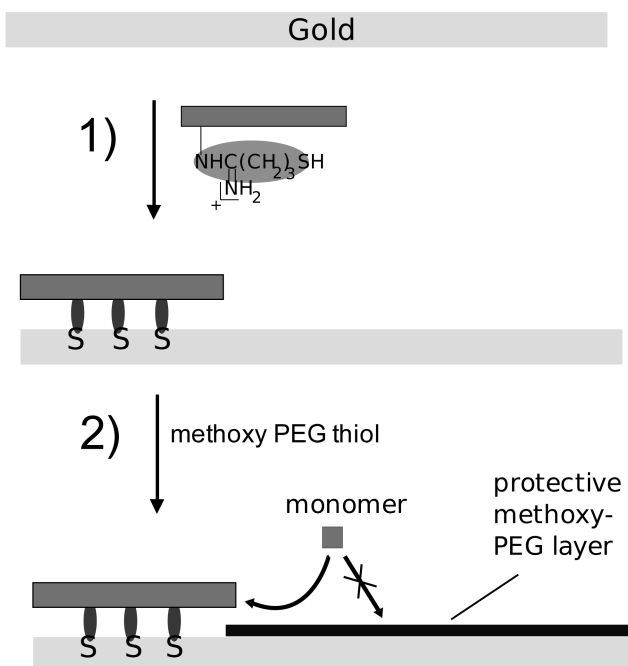


**Figure 5.** Attachment strategy, using 2-iminothiolane (Traut's reagent) to functionalize amyloid fibrils. Pregrown fibrils were incubated with an excess of Traut's reagent (see the Experimental Section for details), and then, the fibrils were attached to gold surfaces. The mass spectrum shows  $\alpha$ -synuclein fibrils functionalized for 15 min and then dissociated by suspension in HCl at pH 1.0. The spectrum shows an 11.3 kDa peak illustrating the truncation of the  $\alpha$ -synuclein sequence (see the Experimental Section for details) that can occur after prolonged time and a series of peaks differing by 84 Da corresponding to the masses of attached 2-iminothiolane molecules after recyclization and loss of ammonia.

unmodified amyloid fibrils to a chemically activated layer of molecules carrying a carboxylic acid group. This strategy has been applied several times successfully with the  $\text{A}\beta$  peptide,<sup>20,21,51</sup> and attachment to glass is also possible by using a similar procedure. We have shown above that the chemical functionalization of amyloid fibrils is a convenient strategy to enable their attachment to gold surfaces. As the surface coverages that can be achieved with a given attachment method can vary strongly, we decided to investigate the applicability of the general approach of covalently modifying amyloid fibrils in such a way that they can be attached to a surface at physiological pH values and so studied under more biologically relevant conditions.

We chose for this purpose a small molecule, 2-iminothiolane ("Traut's reagent"), that has previously been used to introduce thiol groups into monomeric proteins.<sup>49,52</sup> This method is efficient and elegant because it is based on a one-step reaction (Figure 5). This cyclic electrophilic reagent is typically attacked by a nucleophilic amine group of the protein with good yield, resulting in the opening of the ring and the exposure of a free thiol group, ideal for surface attachment. It has been shown, however,<sup>53</sup> that a subsequent reaction can occur that leads to the loss of ammonia and the formation of an N-substituted 2-iminothiolane, a species that is not capable of forming a gold–sulfur bond, a result in accord with studies on alkane sulfides that have been shown to adsorb only noncovalently to gold surfaces, and not to form covalent links as do thiols or disulfides.<sup>54</sup> The half-life of the free thiol form of the attached Traut's reagent that is prone to this type of secondary reaction depends on the nature of the specific amine involved, and on the pH and the temperature of the solution.<sup>53</sup>

In order to test whether this secondary reaction would interfere with our purpose of surface attachment, we studied the interaction of Traut's reagent with fibrils formed from human  $\alpha$ -synuclein and amyloid  $\beta$  (1–42). A high fibril surface coverage, as shown in Figure 6a, was achieved when the gold surface was incubated with fibrils shortly after functionalization (see the Experimental Section), indicating that the recyclization reaction does not occur within minutes and that the free thiol is available for a sufficient amount of time (of the order of 1 h) to ensure covalent attachment to the gold. The finding that a molecule of  $\alpha$ -synuclein can carry several modifications (as can be seen in the cascade of peaks with  $\Delta M = 84$  Da in a mass spectrum of dissociated modified fibrils, Figure 5) is a consequence of the fact that the full length sequence contains 15 lysine residues and a considerable part of the sequence appears not to be in the fibril core.<sup>55</sup> AFM imaging shows in addition that the modified fibrils attached to the surface are essentially identical in morphology to unmodified ones and are still able to elongate after incubation with a solution of unmodified monomer, indicating that the modification does not interfere with the capability of the protein molecules to seed fibril growth (see Figure 6). In these experiments, amyloid fibrils that contained truncated sequences (see Figure 5 and the Experimental Section for details) were found to show no detectable difference in surface attachment, morphology, or seeding efficiency relative to fibrils consisting of full length  $\alpha$ -synuclein; the two types of fibrils behave identically in all experiments carried out in the previous study.

When a large excess of Traut's reagent is used, its hydrolysis product, a thiol, can react with the gold surface, even though it has been shown that the half-life of the intact cyclic compound

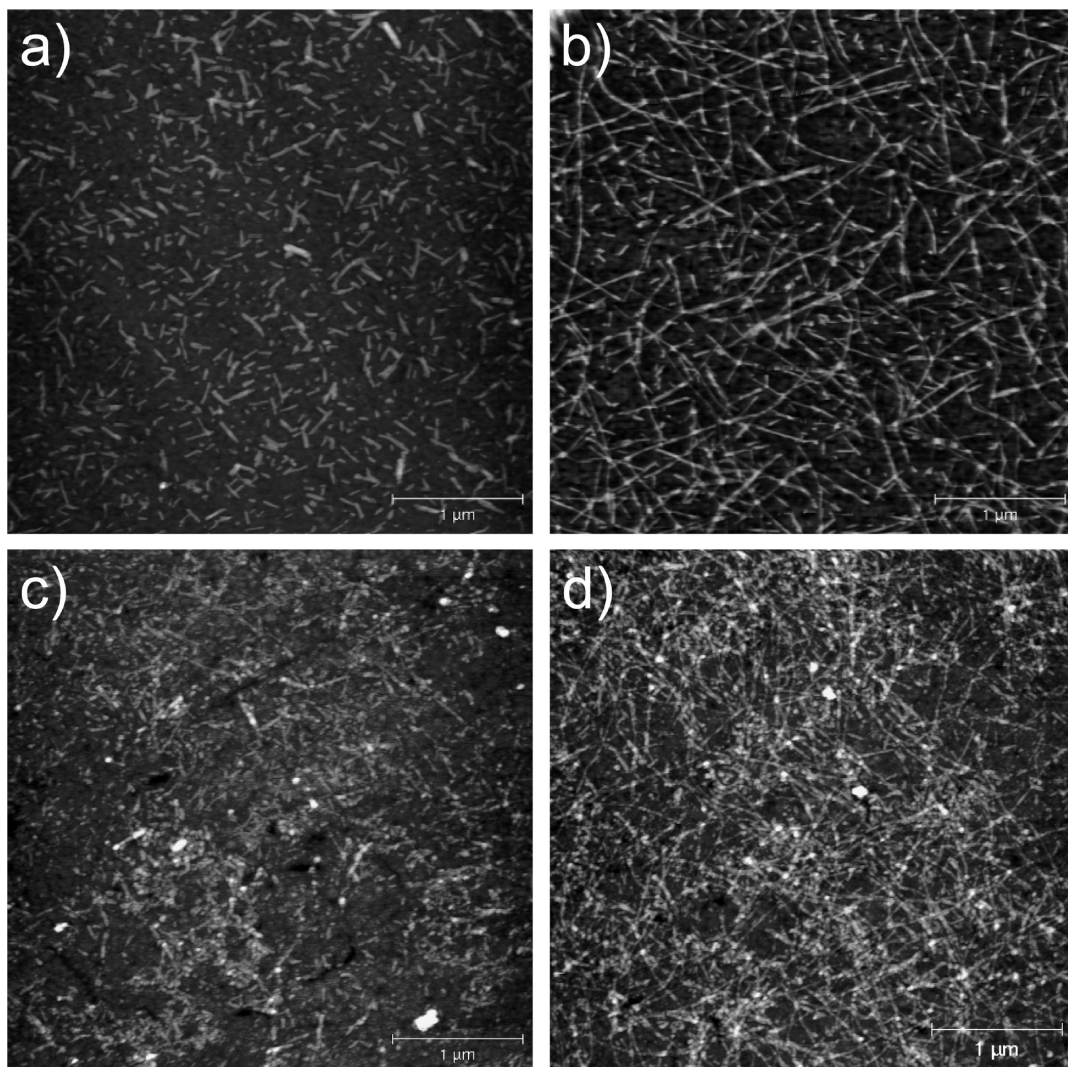


**Figure 6.** AFM images showing short fragments of amyloid fibrils of  $\alpha$ -synuclein (a) and  $A\beta$  (1–42) (c) that were attached to a gold surface via Traut's reagent. The  $\alpha$ -synuclein fibrils were then incubated with a 20  $\mu\text{M}$  solution of monomeric  $\alpha$ -synuclein in PBS for ca. 1 h. The  $A\beta$  fibrils were brought into contact with a 7  $\mu\text{M}$   $A\beta$  monomer solution, also for approximately 1 h. The images demonstrate that, in both cases, the attachment of Traut's reagent did not interfere with the capability of the fibrils to elongate in the presence of monomeric protein.

at neutral pH is several days.<sup>43</sup> Therefore, in order to ensure complete passivation of the surfaces within a much shorter time scale, we incubated the gold surfaces with a methoxy-PEG-thiol after fibril attachment, in a manner analogous to that adopted with the natural cysteine attachment described above. This approach, where pregrown amyloid fibrils were modified with Traut's reagent under physiological conditions, also yielded good results in the case of fibrils formed by the amyloid  $\beta$  (1–42) peptide (Figure 6). As before, no differences in morphology or seeding efficiency were observed compared to fibrils attached via the well established amide coupling to an activated SAM.<sup>20,21,51</sup> In principle, therefore, comparable surface coverages can be achieved with both methods, although the relative mobilities of the activated groups are different. The coupling to an activated SAM requires a high surface density of activated groups, such that the fibrils, which have a limited mobility, will come in contact with such an activated surface group. This requirement no longer applies if the fibrils are able to attach directly to gold via a sulfur-containing linker whenever they come in contact with the surface.

The reactivity of Traut's reagent is very strongly pH dependent, as it relies on reaction with an unprotonated amine group. This reagent is therefore ineffective in modifying fibrils which

are only stable at acidic pH, and another approach is required to achieve efficient functionalization of such structures (e.g., in the case of the B-chain of bovine insulin). This observation prompted us to explore an alternative approach; we modified monomeric peptides at neutral pH with Traut's reagent and then, in a second step, elongated preformed seed fibrils with these modified monomers at acidic pH (see Figure 7a and the Experimental Section). With this method, however, and in contrast to the functionalization of assembled fibrils discussed above, amino acid residues that are crucial to the self-assembly process can be modified and therefore the structure and mechanism of formation of the amyloid fibrils can potentially be altered. Indeed, we find that, in the case of hen lysozyme, the morphology of the fibrils formed from functionalized monomers is different from the morphology of fibrils formed entirely from unmodified proteins (Figure 7c). These differences are highlighted by the finding that some functionalized fibrils (e.g., hen lysozyme fibrils where the monomer had been functionalized with a 3-fold excess of Traut's reagent) wind up into spirals, indicating that the monomer modification introduces strain into the amyloid scaffold, leading to lower persistence length or increased inherent curvature. In many cases, however, the morphology of fibrils grown from functionalized monomers

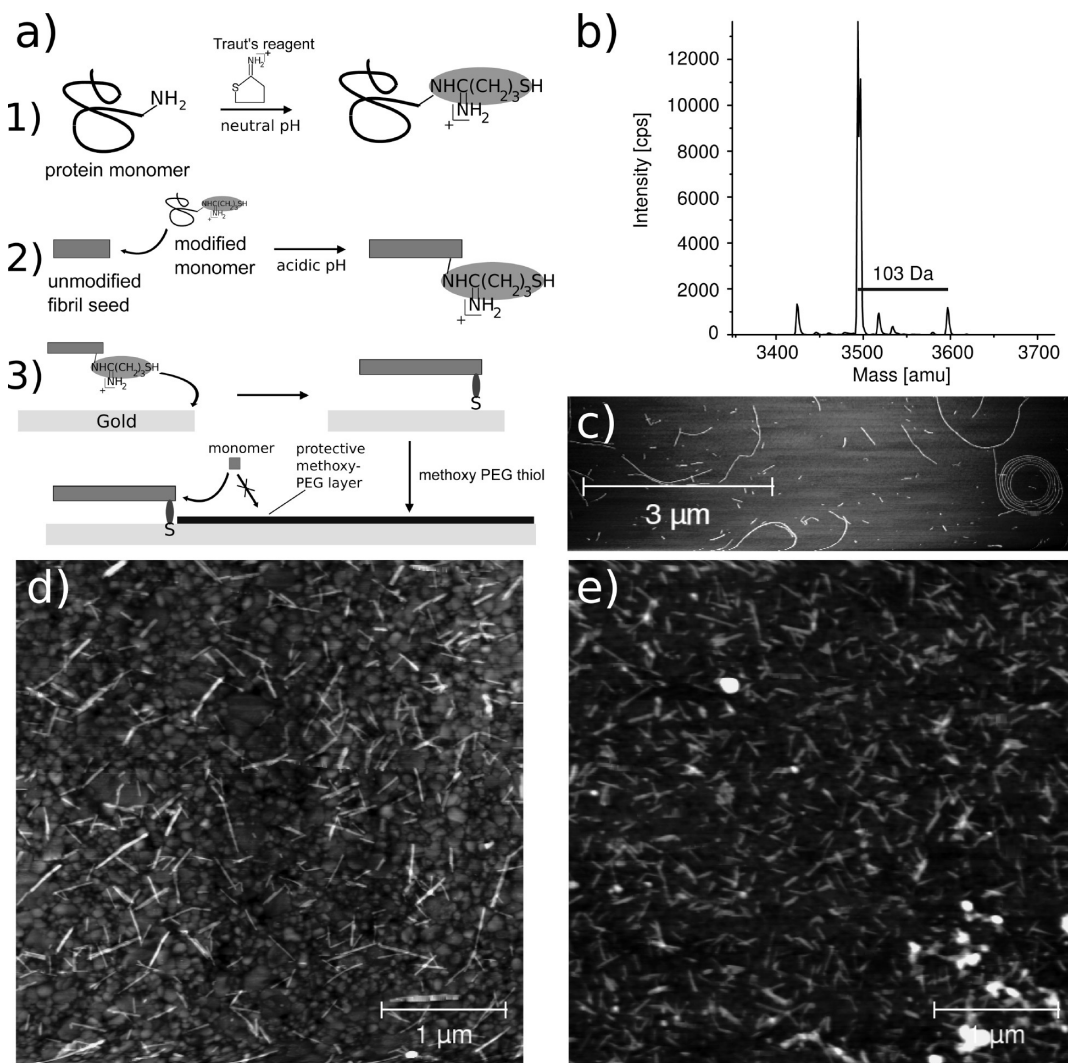


**Figure 7.** (a) Covalent modification strategy involving attachment of Traut's reagent to monomeric protein at neutral pH followed by elongation of pregrown fibril seeds with these modified monomers at acidic pH and then attachment of the modified fibrils to the gold surface. (b) Mass spectrum of the modified B-chain monomers, indicating the small yield of the modification (unmodified monomer around 3500 Da and modified monomer around 3600 Da). Due to the acidification of the peptide solution after incubation with Traut's reagent (see the Experimental Section), Traut's reagent is still intact after more than one day, and has not undergone the subsequent rearrangement reaction described in the text. (c) This strategy, however, can lead to alteration of fibril morphology, as residues crucial for the protein self-assembly can be modified. Figure 1b shows that in the case of hen lysozyme premodification of the monomer can lead to more highly curved fibrils, in extreme cases forming spirals. Despite this potential drawback, this method enabled us to increase very strongly the surface coverage of bovine insulin B-chain fibrils: (c) highest surface coverage achieved with unmodified fibrils; (d) surface coverage achieved with modified fibrils.

is indistinguishable by AFM from unfunctionalized structures; in such cases, this approach represents a very effective strategy to achieve functionality in protein nanostructures. Indeed, using this method, we succeeded in enhancing very significantly the surface coverage of fibrils formed from the B-chain of bovine insulin by 200–300% (compare parts d and e of Figure 7). We analyzed the modified monomers (4-fold excess of Traut's reagent at pH 7.4) by mass spectrometry (Figure 7b) and found that the population of modified monomer (M ca. 3600) is small compared to the population of unmodified monomer (M ca. 3500), similar to the situation where we modified fibrils with cystamine. The Traut's reagent is likely to react with the N-terminus, as this represents the least basic amine within a protein. Therefore, the lack of apparent alterations in the morphology of the structures in this case can be readily understood as a consequence of the small proportion of modified monomers within the final fibrils. A further factor that is likely to reduce the effects of the modification on the filament structure stems from the fact that this modification predominantly occurs

at the extremity of the polypeptide chain which is likely to be less important in the assembly mechanism than a position within the sequence. We note also that, in the mass spectrum acquired for the functionalized insulin B-chain monomer solution, we only observe modified peptides where the attached Traut's reagent has not undergone the subsequent reaction leading to the elimination of ammonia, as shown by the measured masses of M + 103 instead of M + 84. The stability of this functional group is due to the lowering of the pH from 7.4 to 1 (see the Experimental Section) 5 min after the addition of the Traut's reagent, conditions that quench the subsequent rearrangement reaction. This quenching stems from a significant decrease in the population of the thiolate, which is the nucleophile for the intramolecular nucleophilic attack.

In summary, we find that the covalent modification of preformed amyloid fibrils with a small molecule, 2-iminothiolane, under physiological conditions is a very convenient and effective strategy for surface attachment of fibrils formed from the naturally unfolded polypeptides A $\beta$  (1–42) and  $\alpha$ -synuclein.

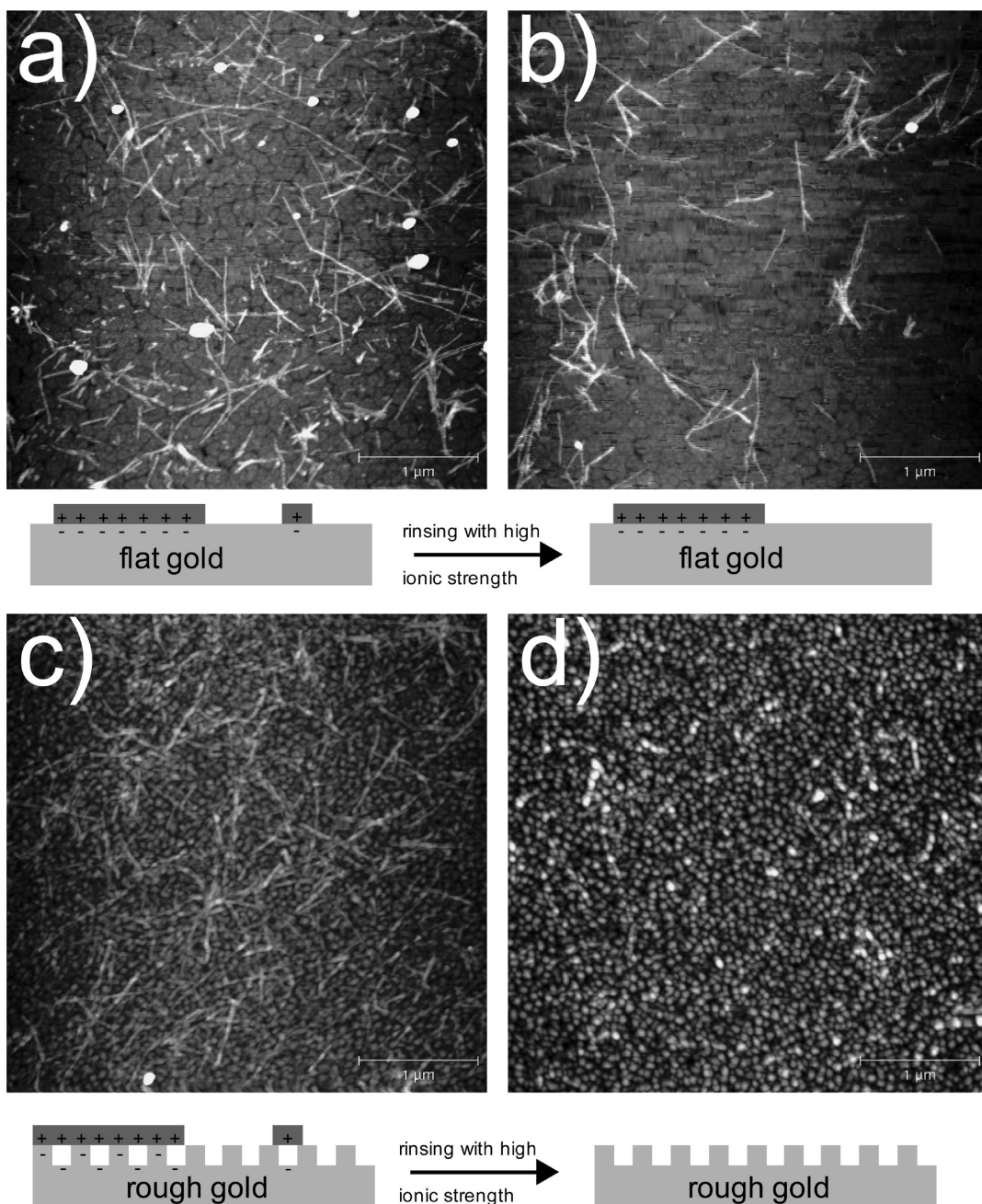


**Figure 8.** Stability of noncovalent interactions between gold surfaces of different roughnesses and PI3K-SH3 amyloid fibrils. In the case of the smooth (rms roughness ca. 0.5 nm) template-stripped gold (top), the difference between rinsing with 10 mM HCl (a) and 10 mM HCl + 100 mM NaCl (b) is small, with only short fibrils in general being removed. However, the interaction forces are weaker in the case of the gold surface with higher roughness (rms roughness ca. 1.5 nm) (bottom). Here, the fibrils were entirely displaced by rinsing the surface with a solution of high ionic strength (compare parts c and d).

The modification is fast and efficient and does not normally alter the morphology or seeding capacity of the amyloid fibrils. Compared to the alternative method of coupling the fibrils to an activated SAM, our strategy involves less steps and can be controlled more accurately through variation of the concentration of Traut's reagent and the incubation time. Therefore, this method is very well suited for an application in surface bound biophysical measurements.

#### Covalent versus Noncovalent Attachment for Applications in Biosensing

Noncovalent interactions between charged molecules and metal surfaces can be strong because of the high polarizability

of metals; a charged compound in contact with a metal surface can induce an opposite (mirror) charge which leads to strong Coulombic attractions.<sup>56</sup> Noncovalent interactions between the soluble forms of proteins and surfaces of different chemistry and topography have been studied in detail, especially in the framework of potential biomedical applications.<sup>57–59</sup> These interactions are likely to play an equally important role in the case of amyloid fibrils, as the protein monomers that form the fibrils are often very highly charged under the acidic denaturing conditions where many proteins most readily form amyloid structures.<sup>33</sup> Figure 8 demonstrates that noncovalent interactions depend on the roughness of the surface by comparing the outcome of incubating of WT PI3K-SH3 fibrils on very smooth

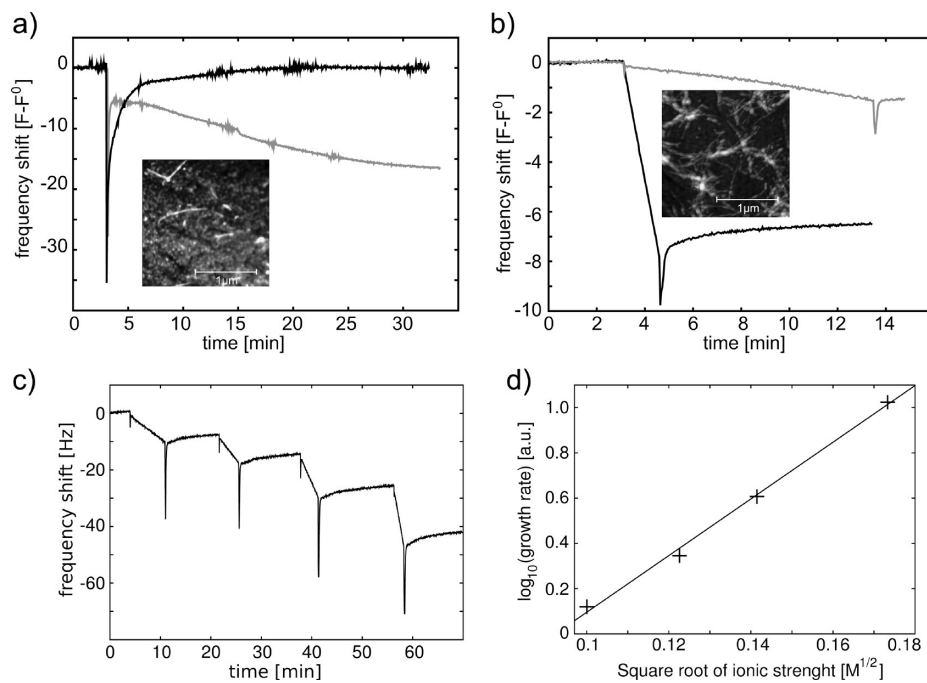


**Figure 9.** QCM measurements of PI3K-SH3 amyloid growth, illustrating the advantages of covalently attaching the fibrils to the biosensor surface. (a) Fibrils have been exposed to PI3K-SH3 monomer solution at pH 2.0: before (gray line) and after (black line) flushing the cell with 40 mM NaCl solution at a flow rate of ca. 10 mL/min. The reversible spike in frequency at  $t = 3$  min is due to the injection of sample into the QCM cell. The frequency shift of the gray line indicates growth of the surface bound fibrils, whereas the absence of a shift in resonant frequency for the black line is characteristic of a lack of any fibril elongation. Indeed, AFM imaging of the chip after the experiment revealed that very few fibrils were left on the surface; the contact of the chip with a solution of moderate ionic strength had removed most of them (see inset). (b) Fibrils covalently attached via the modification scheme of Figure 3. Frequency shift due to fibril elongation in the absence of NaCl (gray line) and in the presence of 20 mM NaCl, after having been flushed repeatedly with solutions of moderate ionic strength (black line). AFM imaging reveals that, at the end of the experiment, after repeated contact with solutions of different salts and of similar ionic strengths as in part a, the surface coverage of fibrils remains high (see inset). The reliable covalent attachment therefore allows for the probing of the influence of ionic strength on the elongation rate: (c) a successive increase in NaCl concentration (0, 5, 10, 20 mM) leads to an increasing rate of amyloid fibril elongation. A plot of the log of the rate constant against the square root of the ionic strength can be used to estimate the effective charge of the protein that leads to an electrostatic barrier for the aggregation reaction (see main text for details).

template-stripped gold<sup>44</sup> (rms roughness ca. 0.5 nm) and on a gold substrate with a roughness comparable to that of commercially available biosensors (rms roughness ca. 1.5 nm). As the fibrils are very stiff<sup>6</sup> and do not necessarily follow the features of a surface, the roughness determines the average distances between the charges and the polarizable surface and, in addition, the larger contact area between the fibrils and the surface with decreased roughness also increases van der Waals attractions and hydrophobic interactions.

We found that rinsing the surface with a solution of high ionic strength ( $\geq 5 \times 10^{-2}$ ) detaches a larger proportion of noncovalently attached fibrils than occurs when rinsing with a solution of lower ionic strength ( $10^{-2}$  M) (Figure 8). This result indicates that the majority of the interaction energy in such cases is likely to result from electrostatic forces. The shear stress  $\sigma = \eta \cdot (\partial u / \partial z)$  experienced by the fibrils during the rinsing can be estimated to be of the order of 1 N/m<sup>2</sup> (assuming maximum shear rates  $\partial u / \partial z$  of 1000 s<sup>-1</sup> and a dynamic viscosity of  $10^{-3}$  Pa s). With a fibril diameter of roughly 10 nm, this leads to a force per unit length of fibril of  $10^{-8}$  N/m. If this value is compared with an order of magnitude estimate of the unscreened electrostatic forces,  $F/l = \lambda q / 4\pi\epsilon_0\epsilon_r r^2 = (n/l)(q^2 / 4\pi\epsilon_0\epsilon_r r^2) \approx (n/l)(2.9 \times 10^{-12} N)$  (where  $l$  is the unit length of the fibril and  $\lambda = Q/l = nq/l$  is the one-dimensional charge density;  $r$  is here taken to be 1 nm), the two opposing forces are only of the same order of magnitude for an unrealistically low charge density of  $10^4$  m<sup>-1</sup>. A realistic charge density can be expected to be at least  $10^5$  times higher than this value, due to the high density of protein molecules within the amyloid fibrils, all of them

carrying several charges. Therefore, the forces due to rinsing will not be sufficient to overcome the unscreened Coulomb attraction. If, however, oppositely charged counterions are present, as is always the case, although in varying quantities depending on the ionic strength of the buffer, these ions can diffuse into close proximity with the fibril/surface interface and thereby reduce the electrostatic forces via a Debye-type screening and the formation of ion pairs. The remaining electrostatic, van der Waals, and hydrophobic forces are then of a comparable order of magnitude as the forces from the mechanical action of rinsing, such that rinsing at high ionic strength is able to remove the fibrils (Figure 8).

It is interesting to note that, in the case of fibrils formed from bovine insulin and its B-chain fragment, the charge density of the two types of fibrils is very similar. The B-chain at pH 2.0 carries the same net charge as the intact protein (i.e., the combined A- and B-chain) assuming that the  $pK_a$  values of all residues are independent of each other, an assumption that is consistent with calculations with the protein  $pK_a$  calculator PROPKA.<sup>60</sup> The presence of two sulfonic acid residues in the oxidized B-chain decreases the charge from +5 to +3 at pH 2.0, but the sequence length of 30 residues compared to 51 in full length insulin and the similar fibril diameters imply that the overall charge density of the B-chain fibrils at acidic pH is likely to be very similar to that of fibrils formed from intact insulin under the same conditions. The large difference between the surface attachment of full length insulin amyloid (Figure 2a) and the isolated B-chain (the highest surface coverage achieved is shown in Figure 7d) can therefore be attributed to

the formation of covalent bonds with the gold surface in the case of full length insulin as a result of the presence of cysteines/disulfides compared to the sulfonic acid residues in the B-chain.

In order to demonstrate and explore further the full advantages of covalent attachment rather than reversible adsorption on a gold surface, we performed a series of QCM experiments (shown in Figure 9), in which we incubated a QCM chip with chemically unmodified PI3K-SH3 fibrils, and measured the elongation of the surface bound fibrils when the chip was brought into contact with a solution containing monomeric PI3K-SH3 at pH 2.0. The solution was then replaced with a 40 mM solution of NaCl (also at pH 2.0), followed by renewed incubation with a monomer solution which revealed no observable increase in mass. AFM imaging of the sensor after the experiment was complete revealed that a large part of the fibrils had been displaced by the solution with increased ionic strength (see inset of Figure 9a). On the other hand, a chip that had been incubated with chemically modified (cystamine attached) PI3K-SH3 fibrils showed an increase in the rate of mass addition upon increase in the ionic strength of the protein monomer solution. Despite the fact that the chip had here also been rinsed several times with salt solutions between the measurements, AFM images showed that the chip was still covered with fibrils after the experiment (inset of Figure 9b).

These results establish therefore that our functionalization strategy is an effective path toward controlling the surface attachments of protein structures. This controlled attachment uniquely allows access to quantitative measurements of the properties and kinetics of reactions that such structures can undergo at surfaces. We illustrate this idea by incubating covalently attached PI3K-SH3 fibrils with a series of solutions of monomeric protein with increasing NaCl concentration. The rate of mass addition, and therefore of amyloid fibril growth, was found to increase with increasing ionic strength (Figure 9d), a trend which is in agreement with earlier qualitative observations on this system.<sup>61</sup> However, the highly quantitative nature of biosensor measurements allows us to analyze this experiment in the framework of the primary kinetic salt effect of ionic reactions.<sup>62</sup> The underlying theory is a combination between the Eyring theory of the activated complex and the Debye–Hückel theory of electrolyte solutions. It predicts according to  $\log_{10} k = B + 1.018 \cdot z_A \cdot z_B \sqrt{I}$  that a plot of the logarithm of the reaction rate constant against the square root of the ionic strength should yield a straight line in the case of ionic reactions. In the case where  $z_A$  and  $z_B$ , the charges of the reacting species, are equal and of the same sign, as in the case of amyloid fibril elongation, we expect an increase in rate with increasing ionic strength. The slope of the above-mentioned plot can be used to determine the effective charge of the reacting species. In the case of PI3-SH3 amyloid formation, we obtain a slope of 12.52, corresponding to an effective charge of +3.5. This is considerably lower than the total charge of the protein calculated from the amino acid sequence at pH 2.0 (+12), indicating that the effective charge of the protein is reduced, e.g., through ion pair formation, and that the electrostatic interactions in the transition state are dominated by only part of the total charge. However, the underlying simplifications required for the derivation of the above stated equation may not all be valid in the case of charged macromolecules. We will discuss this in more detail in the framework of a separate study. In the context of the present study, we simply note that the irreversible attachment of amyloid structures to a biosensor surface allows us to study to high accuracy the influence of varying ionic strength and other parameters on the growth of

these polymers and provides insight into the molecular mechanism of this self-assembly process.

## Conclusion

We have explored in the present study strategies designed to attach protein fibrils to gold surfaces. We have observed that noncovalent interactions between amyloid fibrils and gold surfaces can be strong, particularly if the surface of contact is maximized through low substrate roughness. Even under optimal circumstances, however, this noncovalent attachment strategy may not be sufficiently robust to be useful for experiments where the behavior of a constant ensemble of fibrils needs to be monitored accurately and repeatedly under varying conditions. In order to achieve this objective, we developed a set of chemical modification strategies that allows the reliable and irreversible covalent attachment of amyloid fibrils formed from a variety of proteins at different pH conditions (summarized in Table 1). These strategies involve the chemical modification of pre-grown fibrils that have no naturally occurring cysteine residues in their amino acid sequence with small sulfur containing molecules (cystamine and 2-iminothiolane) in order to allow their linkage to an unmodified gold surface. The results show that this objective can be achieved without interfering detectably with the ability of these modified fibrils to elongate on the surface and therefore to act as seeds for experiments involving their growth. This covalent attachment enables quantitative studies of extraordinary reproducibility to be carried out to probe the nature of amyloid fibrils and the kinetics and mechanisms of their formation. In particular, our procedures enable  $\text{A}\beta$  peptides and  $\alpha$ -synuclein to be attached successfully at physiological pH values, developments that are of particular value in the context of studies of the misfolded states linked to Alzheimer's and Parkinson's disease.

**Acknowledgment.** This work was supported by the UK BBSRC, EPSRC, the Cambridge IRC in Nanotechnology, the Wellcome and Leverhulme Trusts (C.M.D.), Unilever (D.A.W.), and St John's College, Cambridge (T.P.J.K.). We thank Dr. Min Zhou and Asha Bodhun for the mass spectrometric analysis, Dr. Neil Birkett for providing the cysteine mutant of PI3K-SH3, Sarah Shammas for providing  $\text{A}\beta$  (1–42) fibrils, and Simon Attwood for providing the template-stripped gold substrates.

## References and Notes

- (1) Limberis, L.; Magda, J. J.; Stewart, R. *J. Nano Lett.* **2001**, *1*, 277–280.
- (2) Limoges, B.; Saveant, J.-M.; Yazidi, D. *J. Am. Chem. Soc.* **2003**, *125*, 9192–9203.
- (3) Engvall, E.; Jonsson, K.; Perlmann, P. *Biochim. Biophys. Acta* **1971**, *251*, 427–434.
- (4) Qin, M.; Wang, L.-K.; Feng, X.-Z.; Yang, Y.-L.; Wang, R.; Wang, C.; Yu, L.; Shao, B.; Qiao, M.-Q. *Langmuir* **2007**, *23*, 4465–4471.
- (5) White, D. A.; Buell, A. K.; Dobson, C. M.; Welland, M. E.; Knowles, T. P. *J. FEBS Lett.* **2009**, *583*, 2587–2592.
- (6) Knowles, T. P.; Fitzpatrick, A. W.; Meehan, S.; Mott, H. R.; Vendruscolo, M.; Dobson, C. M.; Welland, M. E. *Science* **2007**, *318*, 1900–1903.
- (7) Dobson, C. M. *Biochem. Soc. Symp.* **2001**, *1*–26.
- (8) Bucciantini, M.; Giannoni, E.; Chiti, F.; Baroni, F.; Formigli, L.; Zurdo, J.; Taddei, N.; Ramponi, G.; Dobson, C. M.; Stefani, M. *Nature* **2002**, *416*, 507–511.
- (9) Guijarro, J. I.; Sunde, M.; Jones, J. A.; Campbell, I. D.; Dobson, C. M. *Proc. Natl. Acad. Sci. U.S.A.* **1998**, *95*, 4224–4228.
- (10) Chien, P.; Weissman, J. S.; DePace, A. H. *Annu. Rev. Biochem.* **2004**, *73*, 617–656.
- (11) Fowler, D. M.; Koulov, A. V.; Alory-Jost, C.; Marks, M. S.; Balch, W. E.; Kelly, J. W. *PLoS Biol.* **2006**, *4*, e6.
- (12) Dobson, C. M. *Nature* **2003**, *426*, 884–890.

- (13) Calloni, G.; Lendel, C.; Campioni, S.; Giannini, S.; Glioza, A.; Relini, A.; Vendruscolo, M.; Dobson, C. M.; Salvatella, X.; Chiti, F. *J. Am. Chem. Soc.* **2008**, *130*, 13040–13050.
- (14) Makin, O. S.; Serpell, L. C. *FEBS J.* **2005**, *272*, 5950–5961.
- (15) Jimenez, J. L.; Guijarro, J. I.; Orlova, E.; Zurdo, J.; Dobson, C. M.; Sunde, M.; Saibil, H. R. *EMBO J.* **1999**, *18*, 815–821.
- (16) Smith, J. F.; Knowles, T. P. J.; Dobson, C. M.; MacPhee, C. E.; Welland, M. E. *Proc. Natl. Acad. Sci. U.S.A.* **2006**, *103*, 15806–15811.
- (17) Hawe, A.; Sutter, M.; Jiskoot, W. *Pharm. Res.* **2008**, *25*, 1487–1499.
- (18) Kusumoto, Y.; Lomakin, A.; Teplow, D. B.; Benedek, G. B. *Proc. Natl. Acad. Sci. U.S.A.* **1998**, *95*, 12277–12282.
- (19) Luehrs, T.; Zahn, R.; Wuethrich, K. *J. Mol. Biol.* **2006**, *357*, 833–841.
- (20) Cannon, M. J.; Williams, A. D.; Wetzel, R.; Myszka, D. G. *Anal. Biochem.* **2004**, *328*, 67–75.
- (21) Hu, W.-P.; Chang, G.-L.; Chen, S.-J.; Kuo, Y.-M. *J. Neurosci. Methods* **2006**, *154*, 190–197.
- (22) Knowles, T. P. J.; Shu, W.; Devlin, G. L.; Meehan, S.; Auer, S.; Dobson, C. M.; Welland, M. E. *Proc. Natl. Acad. Sci. U.S.A.* **2007**, *104*, 10016–10021.
- (23) Hovgaard, M. B.; Dong, M.; Otzen, D. E.; Besenbacher, F. *Biophys. J.* **2007**, *93*, 2162–2169.
- (24) Okuno, H.; Mori, K.; Okada, T.; Yokoyama, Y.; Suzuki, H. *Chem. Biol. Drug Des.* **2007**, *69*, 356–361.
- (25) Kotarek, J. A.; Johnson, K. C.; Moss, M. A. *Anal. Biochem.* **2008**, *378*, 15–24.
- (26) Buell, A. K.; Tartaglia, G. G.; Birkett, N. R.; Waudby, C. A.; Vendruscolo, M.; Salvatella, X.; Welland, M. E.; Dobson, C. M.; Knowles, T. P. J. *ChemBioChem* **2009**, *10*, 1309–1312.
- (27) White, D. A.; Buell, A. K.; Dobson, C. M.; Welland, M. E.; Knowles, T. P. J. *FEBS Lett.* **2009**, *583*, 2587–2592.
- (28) Knowles, T. P. J.; Shu, W.; Huber, F.; Lang, H. P.; Gerber, C.; Dobson, C. M.; Welland, M. E. *Nanotechnology* **2008**, *19*, 384007.
- (29) Ku, S. H.; Park, C. B. *Langmuir* **2008**, *24*, 13822–13827.
- (30) Aisenbrey, C.; Borowik, T.; Bystrom, R.; Bokvist, M.; Lindstrom, F.; Misiak, H.; Sani, M.-A.; Grobner, G. *Eur. Biophys. J.* **2008**, *37*, 247–255.
- (31) Bain, C.; Troughton, E.; Tao, Y.-T.; Evall, J.; Whitesides, G.; Nuzzo, R. *J. Am. Chem. Soc.* **1989**, *111*, 321–335.
- (32) Yamaguchi, I.; Hasegawa, K.; Takahashi, N.; Gejyo, F.; Naiki, H. *Biochemistry* **2001**, *40*, 8499–8507.
- (33) Chiti, F.; Dobson, C. M. *Annu. Rev. Biochem.* **2006**, *75*, 333–366.
- (34) Hoyer, W.; Antony, T.; Cherny, D.; Heim, G.; Jovin, T. M.; Subramanian, V. *J. Mol. Biol.* **2002**, *322*, 383–393.
- (35) Fink, A. L. *Acc. Chem. Res.* **2006**, *39*, 628–634.
- (36) Devlin, G. L.; Knowles, T. P. J.; Squires, A.; McCammon, M. G.; Gras, S. L.; Nilsson, M. R.; Robinson, C. V.; Dobson, C. M.; MacPhee, C. E. *J. Mol. Biol.* **2006**, *360*, 497–509.
- (37) Krebs, M. R.; Wilkins, D. K.; Chung, E. W.; Pitkeathly, M. C.; Chamberlain, A. K.; Zurdo, J.; Robinson, C. V.; Dobson, C. M. *J. Mol. Biol.* **2000**, *300*, 541–549.
- (38) Frare, E.; Mossuto, M. F.; de Laureto, P. P.; Dumoulin, M.; Dobson, C. M.; Fontana, A. *J. Mol. Biol.* **2006**, *361*, 551–561.
- (39) Gosai, W. S.; Clark, A. H.; Ross-Murphy, S. B. *Biomacromolecules* **2004**, *5*, 2408–2419.
- (40) Goers, J.; Permyakov, S. E.; Permyakov, E. A.; Uversky, V. N.; Fink, A. L. *Biochemistry* **2002**, *41*, 12546–12551.
- (41) Akkermans, C.; Venema, P.; van der Goot, A. J.; Gruppen, H.; Bakx, E. J.; Boom, R. M.; van der Linden, E. *Biomacromolecules* **2008**, *9*, 1474–1479.
- (42) Mishra, R.; Sorgjerd, K.; Nystrom, S.; Nordigarden, A.; Yu, Y.-C.; Hammarstrom, P. *J. Mol. Biol.* **2007**, *366*, 1029–1044.
- (43) Alagon, A. C.; King, T. P. *Biochemistry* **1980**, *19*, 4341–4345.
- (44) Wagner, P.; Hegner, M.; Guntherodt, H.-J.; Semenza, G. *Langmuir* **1995**, *11*, 3867–3875.
- (45) Love, J. C.; Estroff, L. A.; Kriebel, J. K.; Nuzzo, R. G.; Whitesides, G. M. *Chem. Rev.* **2005**, *105*, 1103–1169.
- (46) Fenter, P.; Eberhardt, A.; Eisenberger, P. *Science* **1994**, *266*, 1216–1218.
- (47) Biebuyck, H. A.; Bain, C. D.; Whitesides, G. M. *Langmuir* **1994**, *10*, 1825–1831.
- (48) Morozova-Roche, L. A.; Zurdo, J.; Spencer, A.; Noppe, W.; Receveur, V.; Archer, D. B.; Joniau, M.; Dobson, C. M. *J. Struct. Biol.* **2000**, *130*, 339–351.
- (49) Jue, R.; Lambert, J. M.; Pierce, L. R.; Traut, R. R. *Biochemistry* **1978**, *17*, 5399–5406.
- (50) Young, T.-H.; Lu, J.-N.; Lin, D.-J.; Chang, C.-L.; Chang, H.-H.; Cheng, L.-P. *Desalination* **2008**, *234*, 134–143.
- (51) Ha, C.; Ryu, J.; Park, C. B. *Biochemistry* **2007**, *46*, 6118–6125.
- (52) Traut, R. R.; Bollen, A.; Sun, T. T.; Hershey, J. W.; Sundberg, J.; Pierce, L. R. *Biochemistry* **1973**, *12*, 3266–3273.
- (53) Singh, R.; Kats, L.; Blaettler, W. A.; Lambert, J. M. *Anal. Biochem.* **1996**, *236*, 114–125.
- (54) Lavrich, D.; Wetterer, S.; Bernasek, S.; Scoles, G. *J. Phys. Chem. B* **1998**, *102* (18), 3456–3465.
- (55) Miake, H.; Mizusawa, H.; Iwatsubo, T.; Hasegawa, M. *J. Biol. Chem.* **2002**, *277*, 19213–19219.
- (56) Mukhopadhyay, G. *Phys. Scr.* **1987**, *36*, 676–688.
- (57) Rechendorff, K.; Hovgaard, M. B.; Foss, M.; Zhdanov, V. P.; Besenbacher, F. *Langmuir* **2006**, *22*, 10885–10888.
- (58) Roach, P.; Farrar, D.; Perry, C. C. *J. Am. Chem. Soc.* **2006**, *128*, 3939–3945.
- (59) Glomm, W. R.; Halskau, O.; Hanneseth, A.-M. D.; Volden, S. *J. Phys. Chem. B* **2007**, *111*, 14329–14345.
- (60) Li, H.; Robertson, A. D.; Jensen, J. H. *Proteins* **2005**, *61*, 704–721.
- (61) Zurdo, J.; Guijarro, J. I.; Jimenez, J. L.; Saibil, H. R.; Dobson, C. M. *J. Mol. Biol.* **2001**, *311*, 325–340.
- (62) Moore, W. J. *Physical Chemistry*, 4th edition; Prentice-Hall College Div: 1972.

JP101579N